Atmospheric Environment 243 (2020) 117846

Contents lists available at ScienceDirect

Atmospheric Environment

journal homepage: http://www.elsevier.com/locate/atmosenv

Interpretation of decadal-scale ozone production efficiency in the Seoul Metropolitan Area: Implication for ozone abatement

Lim-Seok Chang [a,**], Jin-Young Choi [a], Jongseok Son [a], Sangbo Lee [a], Daegyun Lee [a], Yu-Jin Jo [b], Cheol-Hee Kim [b,*]

[a] Climate and Air Quality Research Department, National Institute of Environmental Research, Incheon, Republic of Korea
[b] Department of Atmospheric Sciences, Pusan National University, Busan, Republic of Korea

HIGHLIGHTS

- O_x was examined in Seoul Metropolitan Area (SMA) by employing OPEx.
- Local photochemical O_x production and background contribution was separated in SMA.
- Regional background to O_x by about 66 ± 11% in SMA.
- A significant cut in NO_x or in both NO_x and VOC emission was suggested.

ARTICLE INFO

Keywords:
Urban ozone
Ozone production efficiency
Wind direction
VOC/NOx ratio

ABSTRACT

Understanding the drivers of urban ozone (O_3) formation is challenging and requires uncovering the non-linear relationship between O_3 and its precursors. We used a novel method to differentiate between background O_3 levels and local photochemical O_3 generation using the observation-based O_3 production efficiency (OPE) from decade-long observations including nitrogen dioxide (NO_2), nitrogen monoxide (NO), reactive nitrogen compounds (NO_y), O_3, and 56 volatile organic compounds (VOCs) covering eight years (2009–2016). In this study, we employed O_x (=O_3+NO_2), and defined OPE_x as the number of O_x molecules produced from the oxidation of a single NO_x molecule, and estimates the local contribution (in %) to total O_3 from the slope of the O_x−NO_z(=NO_y–NO_x) linear regression. We thus identified the local urban O_3 formation regime using the relationship of several factors, including nitrogen oxide (NO_x), VOC/NO_x, NO_2, NO_z, and long-range transported O_x, and suggested how O_3 can be reduced in the Seoul Metropolitan Area (SMA).

The results show that the regional background dominates the annual level of O_x with a contribution of about 66 ± 11%, while photochemical production acts as a stronger factor influencing the annual variability of Ox than regional background. Regional background varies by transport evidenced by its good correlation with the west wind fraction, whereas photochemical production depends on the VOC/NO_x ratio, which is high in summer and low in winter. The relationship between photochemical production and VOC/NO_x indicates that the transition of the O_x formation regime occurs at a VOC/NO_x ratio of approximately 4 in the SMA. Urban environments with NO_x > 20 ppb typically lie in low VOC/NO_x zone, where reduced NO_2 emissions lead to decreased NO_z but increased OPE_x, with no discernible change in photochemical O_x production. Thus, NO_x emission reductions in urban environments would have a negligible effect on O_x reduction. In contrast, suburban environments such as usually NO_x < 10 ppb are located in the higher VOC/NOx zone, where decreased NO_2 leads to decreased OPE_x with no discernible change in NO_z, consequently suppressing photochemical O_x production. Together, these results suggest that any urban O_3 policy in the SMA should consider significant cuts in NO_x emissions to allow the O_3 regime to shift. The OPEx method can also be applied to other urban areas for the development of effective O_3 reduction policies.

* Corresponding author.
** Corresponding author.
E-mail addresses: lschang@korea.kr (L.-S. Chang), chkim2@pusan.ac.kr (C.-H. Kim).

https://doi.org/10.1016/j.atmosenv.2020.117846
Received 20 April 2020; Received in revised form 5 July 2020; Accepted 3 August 2020
Available online 16 August 2020

1. Introduction

High ozone (O_3) concentrations have adverse effects on human and ecosystem health. Ground-level O_3 causes respiratory and cardiovascular diseases, reduces agricultural production, and limits plant growth (US Environmental Protection Agency, 2006). Following the occurrence of high O_3 levels during record-breaking heat waves in 1994, the Korean government introduced an O_3 alarm system in the following year, an O_3 forecast system in 1997, and also implemented emission control policies aimed at reducing the incidence of high O_3 levels. However, these measures have not been successful in reversing or easing increasing O_3 trends. O_3 levels in the Seoul Metropolitan Area (SMA) showed an upward trend of 3 ppb/yr from 1999 to 2011 (Han et al., 2013), while urban O_3 levels increased by 0.60 ppb/yr from 1998 to 2016 (Kim et al., 2018). Such increasing trends have been commonly observed across East Asia. For example, O_3 levels in Beijing increased by 1.1 ± 0.5 ppb/yr during 2001–2006 (Tang et al., 2009), and 217 sites in East Asia had an average increase of 0.45 ppb/yr in urban daytime O_3 levels over a 15-year period (2000–2014) (Chang et al., 2017).

Urban O_3 is mainly produced as a result of a complex set of reactions that involves volatile organic compounds (VOCs), and oxidization process of nitrogen dioxide (NO_2) and nitrogen monoxide (NO) (Haagen--Smit et al., 1953; Sadanaga et al., 2003). Due to the non-linear relationship between O_3 production and its precursors, O_3 mitigation strategies have prioritized the target precursor based on the developed O_3 isopleth plot for the given area (NRC, 1991; European Commission, 1999; Mazzuca et al., 2016). However, this strategy has not been completely successful as the relationship between O_3 and its precursors is more complicated in the real atmosphere (Sillman, 1993; Friedrich et al., 2000). As a result, various efforts have been made in modeling and measurement studies for the development of control strategies over SMA (Oak et al., 2019; Kim et al., 2005; Na and Kim, 2001; Kim et al., 2009; Choi et al., 2014). However, despite the recent consistent decrease in VOC emissions in the SMA, known as VOC-limited condition (Lee and Hwang, 2005; Susaya et al., 2013) by approximately 31% from 2007 to 2016 (NAPES, 2016), the annual mean O_3 concentration increased substantially by 49% over the same period. In addition, it has been reported that if NO_x (=NO + NO_2) decreases under VOC-sensitive conditions, O_3 levels may further increase (Jacob, 1995; Marr and Harley, 2002). One of the causes of this uncertain diagnosis is the unavailability or lack of sufficient VOC observations, thus limiting confidence in previous O_3 abatements.

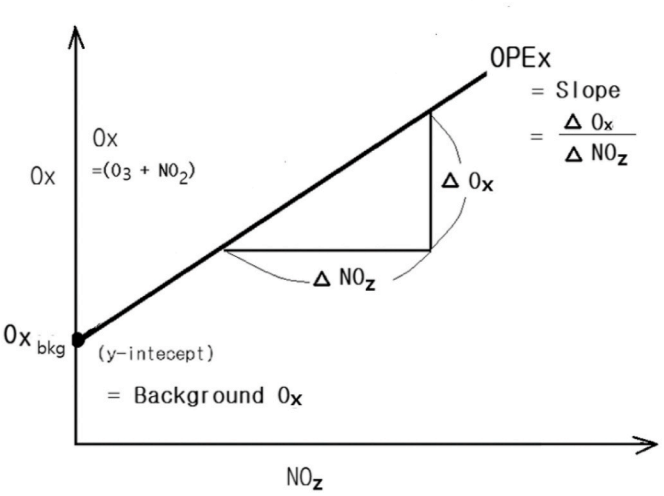

Fig. 2. Schematic diagram of OPE_x estimation using the slope of O_x–NO_z.

The OPE is defined as the number of O_3 molecules produced from the oxidation of a single NO_x molecule. The OPE allows differentiation between photochemically produced O_3 and regional background O_3. Therefore, OPE and its relevant information such as the relationship of O_3 with main atmospheric factors, known as controlling O_3 variability, are the useful tools for developing future national emission control policies and assessing their effectiveness.

A number of studies have applied OPE to investigate the origin of O_3 pollution. Zanis et al. (2007) applied OPE to the lower free atmosphere, stressing the role of photochemical O_3 production during the O_3 spring maximum, whereas Hirsch et al. (1996) applied it to a Harvard forest, attributing an O_3 concentration peak during May–June to background O_3. Over the Northeast Asia, the OPE was also applied using long-term

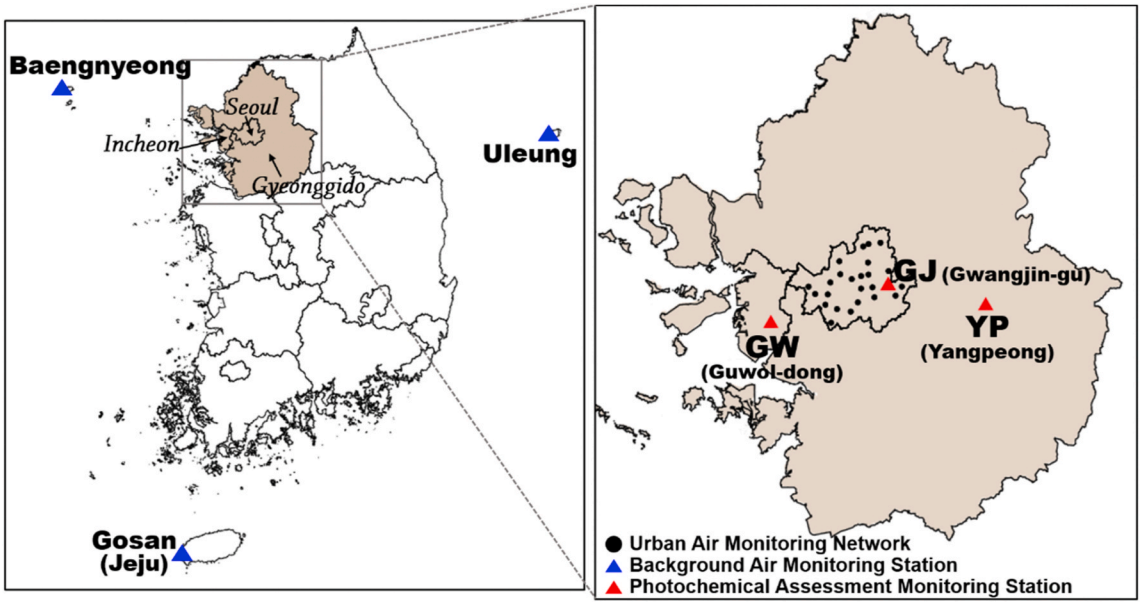

Fig. 1. Locations of air monitoring networks over Seoul metropolitan area (SMA). Twenty-five Urban Air Monitoring Network (UAMN) in Seoul, three National Background Monitoring Network (NBMN), and three Photochemical Assessment Monitoring Station (PAMS) selected for this study, are indicated by filled black circles, blue triangles, and red triangles, respectively. (For interpretation of the references to colour in this figure legend, the reader is referred to the Web version of this article.)

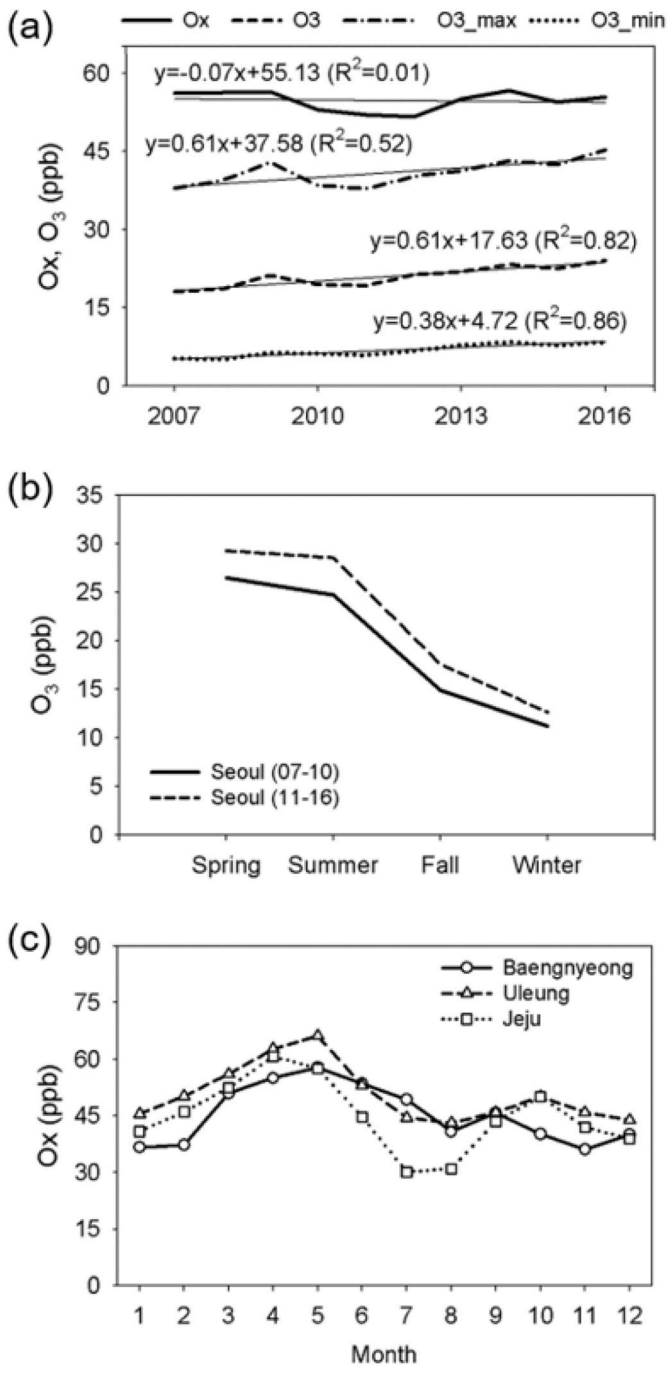

Fig. 3. (a) Annual variations in O_x, O_3, daily maximum, and daily minimum O_3 concentrations; (b) seasonal variations in O_3 in Seoul for 2007–2016; (c) seasonal variations in O_x at the three background sites averaged over different years depending on data availability. The values for Seoul were obtained from 25 sites of the Urban Air Monitoring Network.

observation data. Ge et al. (2012) studied the cause of elevated summer O_3 levels at Shangdianzi by OPE analysis.

To elucidate urban O_x (=O_3+NO_2) response to precursor variations in the SMA, we used decade-long NO_x, O_3, and VOC observations (for 56 VOCs), and applied these data to the O_3 production efficiency (OPE) to better understand the relationship between several factors such as VOC/NO_x ratio, reactive nitrogen compounds NO_y, NO_z, (=NO_y–NO_x), and long-range transport fractions. In this study, we employed OPE and identified the local urban O_3 formation using the relationship of several factors, including VOC/NO_x, NO_y, NO_z and long-range transported O_x, and suggested how O_3 can be reduced in SMA.

2. Methods and data

2.1. Datasets

The data used in the present study were collected from Korean Ministry of Environment Photochemical Assessment Monitoring Station (PAMS), National Background Monitoring Network (NBMN), and Urban Air Monitoring Network (UAMN), as shown in Fig. 1. The PAMS were first established in regions with high O_3 levels in early 2000. Data collected at PAMS are used to monitor VOCs that contribute to O_3 production and to obtain baseline data for establishing effective O_3 management measures. By 2016, eight PAMS sites were in operation over SMA where O_3 levels. The NBMN is in operation on islands on three sides of the Korean Peninsula (Baengnyeongdo, Jejudo, and Ulleungdo), and UAMN's 25 sites in Seoul were in operation within the SMA by 2016 (Fig. 1). Here, UAMN was used to diagnose the long-term O_3 trends (session 3.2), and PAMS and NMBN was employed for OPE estimation (session 3.3).

The UAMN and NBMN collect hourly NO_2 and O_3 concentration data, while the PAMS collect NO_y, NO, O_3, and VOC concentration data. Ultraviolet (UV) photometry, chemiluminescence, and automatic gas chromatography methods were used to measure the concentrations of O_3, NO_2, and 56 VOC species, respectively. Both NO_y and NO were measured using chemiluminescence, and NO_2 was measured by going through a molybdenum converter. As NO_2 is partially oxidized to NO_z by the molybdenum converter, we detracted up to 10% from the NO_2 concentration as appropriate. Given the uncertainty that exists, therefore our results should be taken into account a degree of such uncertainties relevant to the NO_2 measurement. The sampling protocol, measurement methods, and quality assurance/quality control procedures indicated in Table S1 (Han et al., 2000), and are in accordance with the Standard Operating Procedure of Air Pollution by the Ministry of Environment of Korea (http://webbook.me.go.kr/DLi-File/NIER/09/023/5641953.pdf).

Among eight PAMS sites in the SMA, three target sites were selected for this study, where simultaneous observations for NO_2, NO, O_3, NO_y, NO, and 56 VOC species were all available at the same time. Table S2 lists the observed 56 species of VOCs, and Fig. 1 shows both 25 UAMN sites located in Seoul, and the three selected PAMS sites within the SMA: Gwangjin-gu (GJ), Incheon Guwol-dong (GW), and Gyeonggi-do Yangpyeong-si (YP). GJ is located in the center of the metropolitan area and is characterized by heavy traffic. Incheon GW has scattered industrial complexes and is located upwind from Seoul. YP is distant enough from areas of heavy traffic that it is used for monitoring the discharge of photochemical products from the metropolitan area. The monitoring period differed for the PAMS site: 8 years (2009–2016) for GJ, 6 years (2011–2016) for GW, and 7 years (2010–2016) for YP. Three MBNM monitoring sites representing the background regions of three ocean sides of Korean Peninsula (Baengnyeongdo, Jejudo, and Ulleungdo) were also used for comparison with the regional background O_3 levels estimated from OPE analysis.

2.2. Methods

The OPE is conventionally calculated from the linear regression between O_3 and NO_z, and is useful for understanding O_3 production on a regional scale (Hirsch et al., 1996) and the response to precursor emission controls (Lei et al., 2007). In this study, O_x (= O_3 + NO_2) was used instead of O_3, as employed previously (Chou et al., 2009) for OPE estimation. Thus in this study, OPE_x (OPE using O_x instead of O_3) was used hereafter. The advantages of this substitution are that the titration effect of NO_2 can be eliminated, and NO_2 emission resulting from HNO_3 formation can be reduced, thereby leading to a more precise representation of the actual photochemistry.

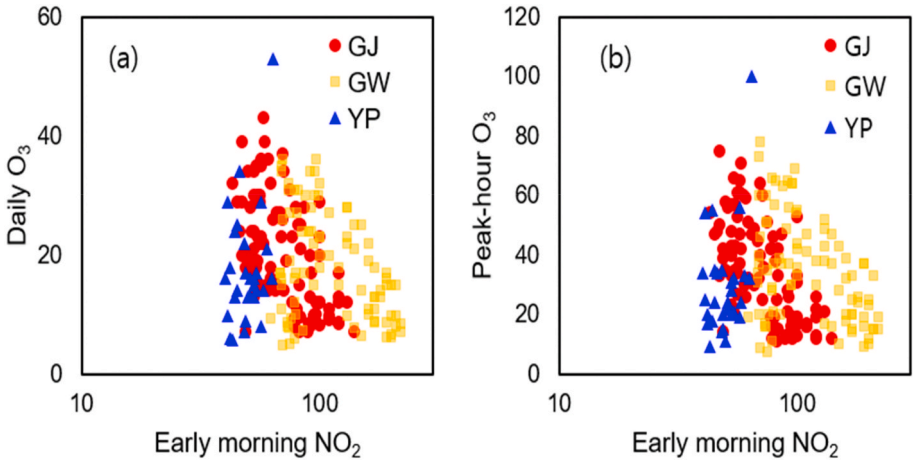

Fig. 4. Scatter diagram of (a) daily mean and (b) peak-hour (1200–1600 local time) O_3 concentrations against early-morning-hour (0600–0900 local time) NO_2 concentrations for 2007–2016 at Gwangjin (GJ), Guwol (GW), and Yangpeong (YP).

We estimated OPEx on days when the following two criteria were met. First, simultaneous measurements of O_3, NO_y, NO, and NO_2 had to be available for at least a 7-h period between 0900 and 1700 local time. Second, the linear correlation coefficient (R) between O_x and NO_z had to be greater than 0.7, respectively, during 2009–2016. The first criterion is for checking basic data availability, and the second criterion is to select only daytime data when the photochemical reaction occurred with lower meteorological impact. The selected numbers are approximately 15%, 16%, and 35% of the days that satisfied criterion 1 and 2, respectively.

Photochemical production of O_x (ΔO_x) is obtained by multiplying OPE_x with NO_z, whereas the regional background O_x (O_{x_bkg}) is defined as the y-intercept of the regression line between O_x and NO_z, as indicated in Fig. 2. All NO_z was assumed to have originated from NO_x oxidation (Zanis et al., 2007). In this process, we therefore estimated OPE_x on days when the following two criteria were met. First, simultaneous measurements of O_3, NO_y, NO, and NO_2 had to be available for at least a 7-h period between 0900 and 1700 local time. Second, the linear correlation coefficient (R) between O_x and NO_z had to be greater than 0.7. These numbers equate to 15%, 16%, and 35% of the days that satisfied criterion 1, respectively.

To estimate the contribution to O_x variability from two main factors: ΔO_x and O_{x_bkg}, the fluctuations of these factors were quantified by dividing the doubled standard deviation by the mean concentration of O_x ($2\sigma/m$) for the corresponding period. This value accounts for 95% of the overall O_x variability. Here σ and m represent the mean and standard deviation, respectively.

3. Results and discussion

3.1. Characteristics of O_3 in the Seoul Metropolitan Area

Fig. 3 showed the annual mean O_3 concentrations averaged over 25 sites of UAMN located within Seoul (indicated in Fig. 1). Over the past decade (2007–2016) the annual mean O_3 concentrations steadily increased at a rate of 0.61 ppb/yr (Fig. 3a), which is significantly higher than the daytime O_3 level increasing rate in East Asia during 2000–2014 (0.45 ppb/yr) (Chang et al., 2017). Daily peak O_3 is believed to have caused an increase in the daily mean O_3 during this season (see O_3_max in Fig. 3a), as also shown in Han et al. (2013). Statistical summary of annual O_3 trends of was listed in Table S3. In Fig. 3b, the O_3 increases are observed in spring and summer. It should be noted that in monthly analysis O_3 observation was the highest in May–June, representing intraseasonal features in SMA (not shown).

Meanwhile, the O_x level in Seoul shows no significant trend in the last decade (Fig. 3a and Table S3). The main cause for this behavior is the trade-off between increased O_3 and decreased NO_2 concentrations, because O_3 is interchangeable with NO_2 in photochemical reactions.

The O_3 formation regime is a major indicator for O_3 pollution characteristics in a region. To identify the O_3 formation regime, we used the relation between NO_x emission and the peak O_3 level. In the current study the NO_2 mixing ratio in the early morning hours is used as a proxy for NO_x emissions, as previously employed (Godowitch et al., 2010). Regarding the regime categorization, a regime is classified as VOC-limited when NO_2 during the early morning hours (0600–0900 local time) is in a negative correlation with the peak-hour (1200–1600 local time) O_3 level only, while a NO_x-titration regime exists when NO_2 is in a negative correlation with both peak- and non-peak-hour (0600–1200, 1600–1700 local time) O_3 (Li et al., 2016). Under the VOC-limited regime, a decrease in NO_2 reduces the O_3 level during peak hours but increases the O_3 level during non-peak hours. The correlation analysis categorizes Seoul as a NO_x-titration region, but prevents regime determination for Incheon due to the lack of a clear trend in the annual NO_2 level. Fig. 4 shows scatter plots for both peak-hour O_3 and early morning NO_2 for three areas (GW, GJ, and YP). As in Fig. 4, a negative correlation between O_3 and morning-hour NO_2 was found in GJ. The correlation for YP is opposite to that for GJ, while GW shows no distinct features. Thus, GJ can be classified as a NO_x-titrated regime, GW as a VOC-limited regime (Lee and Hwang, 2005; Han et al., 2013), and YP as a NO_x-limited regime. When we apply the O_3–NO_2 correlation averaged over all UAMN sites in Seoul, Seoul is categorized as a NO_x-titration region.

3.2. O_x variations and background vs. local photochemical O_x

3.2.1. Seasonal O_x variation

The O_x observations at the three PAMS sites are divided into photochemically produced O_x (ΔO_x) and regional background O_x (O_{x_bkg}) with the help of OPE_x, and seasonal and annual characteristics of both ΔO_x and O_{x_bkg} are examined in this section. Fig. 5 shows the seasonal variations of monthly mean O_x, O_{x_bkg}, ΔO_x, and frequency for days selected based on the criteria described in the Methods section. Two apparent peaks in O_x and O_{x_bkg} can be observed with a main peak in May and a secondary peak in September–October. Concentrations of O_{x_bkg} decreased from 47 to 76 ppb during April–June to 30 ppb in August. This seasonal variation of O_{x_bkg} is consistent with that at the background sites of Baengnyeongdo, Jejudo, and Ulleungdo (Fig. 3c). The level of ΔO_x is low in February but begins to increase in March and reaches a peak in May (Fig. 5), representing a dry summer maximum and wintertime minimum. The shift of the O_x peak from that of O_{x_bkg} is

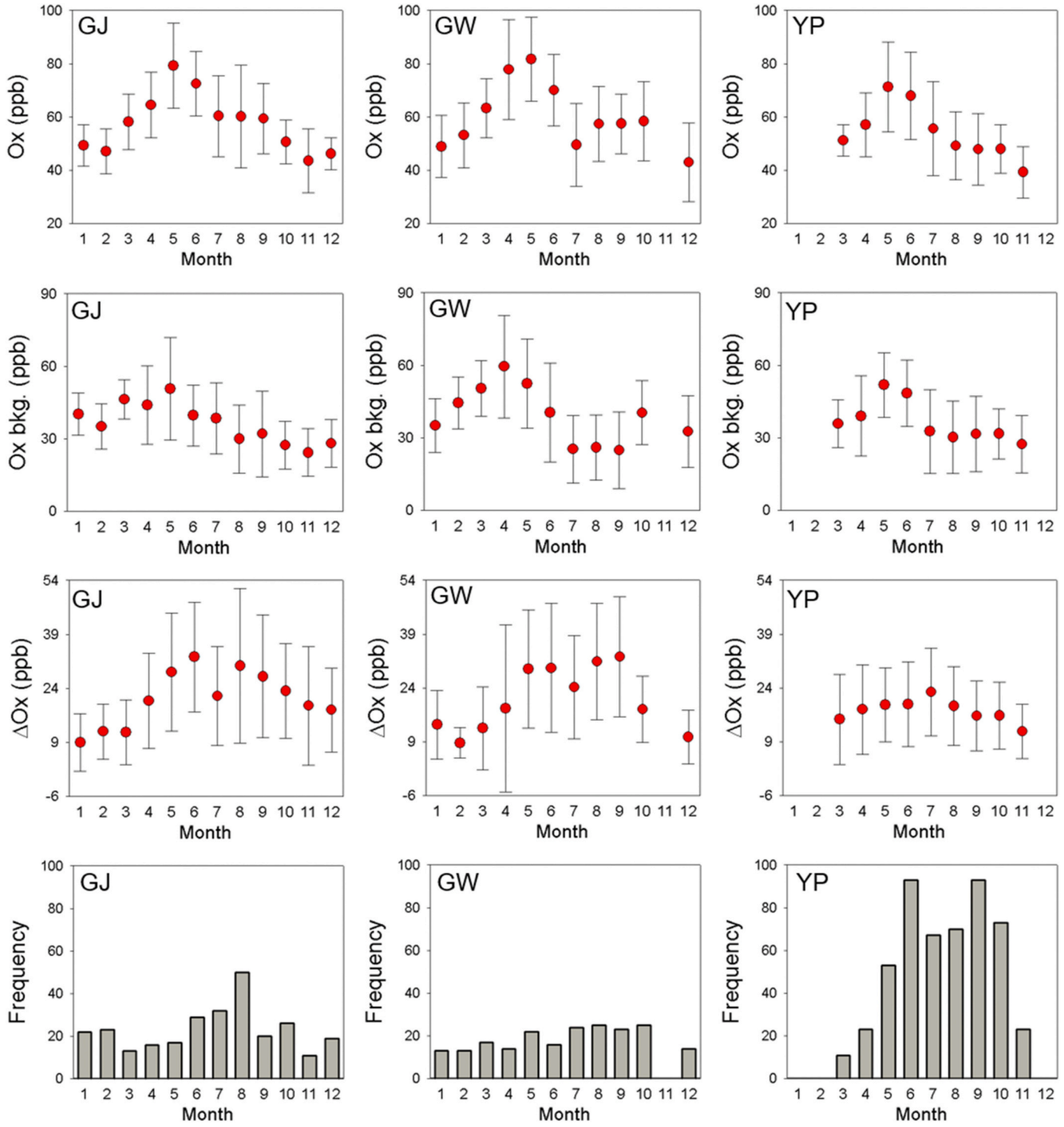

Fig. 5. Seasonal variations in monthly mean O_x (upper panel), O_{x_bkg} (upper middle panel), and ΔO_x (lower middle panel) at Gwangjin (GJ) (left), Guwol (GW) (middle), and Yangpeong (YP) (right) during the study period. The study period is 2009–2016 for GJ, 2011–2016 for GW, and 2010–2016 for YP. Error bars for the monthly mean O_x, O_x_bkg, and ΔO_x denote 95% confidence intervals. The frequency of the days selected following the criteria described in the methods section is illustrated by grey column bars (lower panel).

caused by an increase in ΔO_x toward summer. The annual total mean concentrations of regional background O_{x_bkg} dominate with a contribution of about 66 ± 11% to the level of O_x.

Values for ΔO_x are determined by definition of OPE_x, such as $\Delta O_x = OPE_x \times \Delta NO_z$, as illustrated in Fig. 2. At GJ, the seasonal variation in ΔO_x appears to be in phase with OPE_x, while it aligns with NO_z at YP (Fig. 6). As shown in Fig. 6, GJ exhibits a convex shape for OPE_x, whereas YP exhibits a concave shape. The OPE_x level reaches a peak of 4–8 in summer and decreases to 1–2 in winter at GJ, which is similar to values reported for the urban area of Phoenix in the US (2–7) (Kleinman et al., 1994) and those modeled for Mexico City (4–12) (Lei et al., 2007). For NO_z, a concave pattern is observed at GJ, whereas a convex pattern exists at YP (Fig. 5). This pattern suggests that OPE_x is a main driver of seasonal variation in ΔO_x at GJ, whereas NO_z is an important controlling factor at YP.

Fig. 7 illustrates the seasonal variations in VOC/NO_x ratios and OPE_x

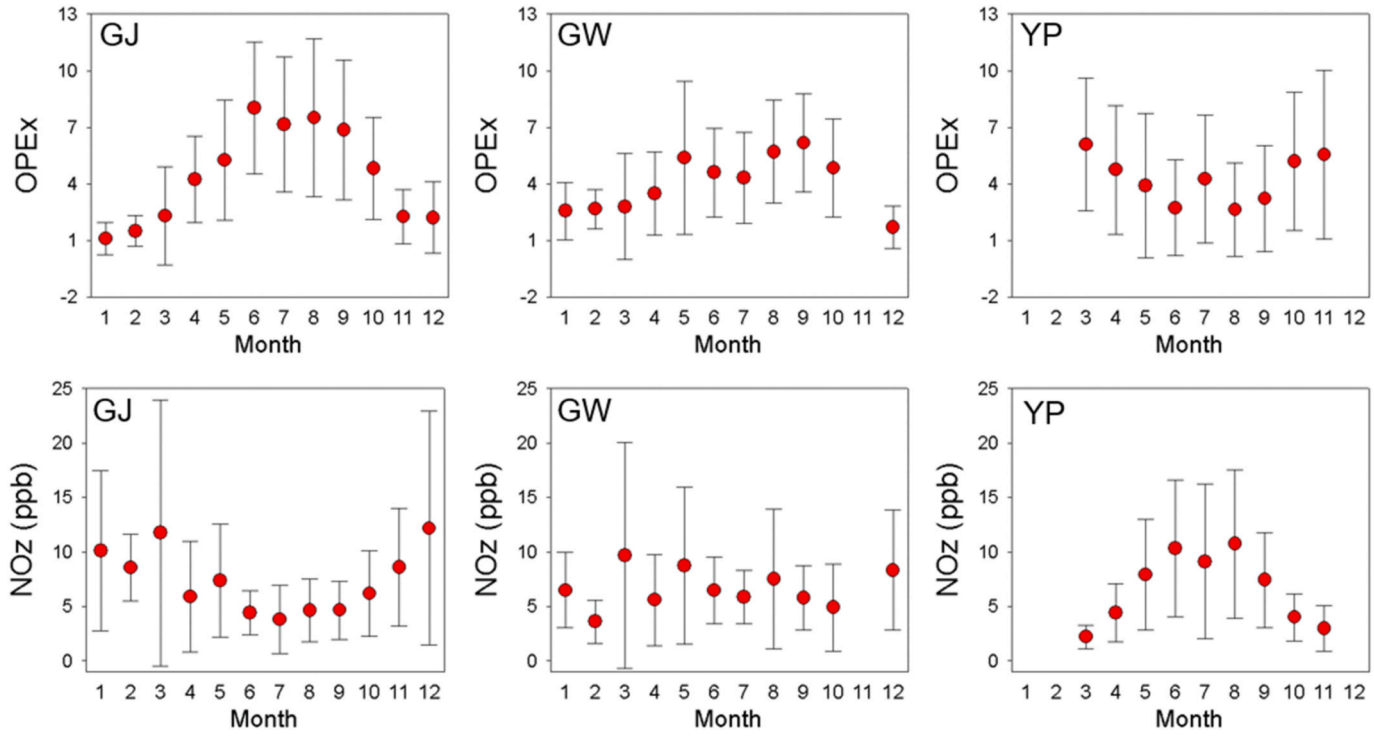

Fig. 6. Same as described for Fig. 5, but for OPE_x and NO_z.

at the three PAMS sites. OPE_x is influenced by several factors: VOC/NO_x, UV radiation, water vapor, and other factors (Zanis et al., 2007), and among them VOC/NO_x is one of the most important factors controlling OPE_x (NRC, 1991). The ratio of VOC/NO_x shows relatively higher in summer than in winter (Fig. 7a). Although there are higher VOC patterns in summer in GJ and GW, which might be evident for isoprene, one of the biogenic VOC species with a strong photochemical O_3 creation potential (POCP) (Bowman and Seinfeld, 1994), there exists no unique variation in total VOC level at all three sites while NO_x showed rather distinct seasonal variations: higher in winter and lower in summer; yielded the winter-low (but not distinctive) variations of VOC/NO_x (Fig. 7a). As a result, OPE_x has a positive correlation with VOC/NO_x at GJ and GW, whereas it has a negative correlation at YP. The convex shape for VOC/NO_x at GJ and GW is caused by a stronger seasonal variation of NO_x than that of VOC (Fig. 7b and c); NO_x dominates VOC in winter mainly due to the increased domestic heating and vehicle NO_x emissions.

3.2.2. *Annual O_x variations*

We chose the O_3 peak months of April–June as a representative period to account for annual O_x variations. Because the number of days per year that meet the criteria were inhomogeneous over the study period, the O_x averaged over the representative period shows no statistically significant trend at the three PAMS sites.

Fig. 8 shows the annual variations in O_x, O_{x_bkg}, and ΔO_x at the three PAMS sites during the study period. Note that "$O_x = O_{x\_bkg} + \Delta O_x$." In Fig. 8, the proportion of O_{x_bkg} is higher than that of ΔO_x in the O_x levels at the three sites, whereas the proportion of ΔO_x is higher than that of O_{x_bkg} in O_x variability. The contribution of ΔO_x to O_x is, on average, approximately 34% at the three sites, which is similar to the modeled values for Korea, for example 28–38% (Chou et al., 2009), 22.8–34.8% (Nagashima et al., 2010), and 5–20% (Li et al., 2016).

As shown in Fig. 9a, the annual mean OPE_x shows a reasonable correlation with VOC/NO_x ratio in GJ and GW, indicating that VOC/NO_x is a main factor controlling OPE_x in two sites. On the other hand, lower correlation between OPE_x and VOC/NO_x ratio in YP where there are high VOC/NO_x ratios. The optimum VOC/NO_x ratio, at which a maximum amount of O_3 is produced, seems to be around 4 in GJ and GW, whereas it is below 4 at YP, all of which are smaller than that derived from a typical O_3 isopleth used in EPA's Empirical Kinetic Modeling Approach (EKMA) (NRC, 1991). Fig. 9a shows that GJ and GW are typically areas with low VOC/NOx conditions, while YP is an area characterized by high VOC/NOx conditions. Under the condition of a low VOC/NO_x ratio, a decrease in NO_x concentration favors O_3 formation by retarding the $OH–NO_2$ reaction to remove OH and NO_2 through the photochemical chain. In contrast, under high VOC/NO_x conditions, a decrease in NO_x retards O_3 formation by favoring peroxy–peroxy reactions to remove radicals from the chain.

To examine the effects of long-range transport (LRT) on regional background O_3, we analyzed the correlation between wind direction and regional background O_3. It is assumed that pollution sources are located on the windward side of the three sites under dominant westerly winds in mid-latitude. The west wind fraction (WWF) is defined as the degree to which westerly wind is dominant over easterly wind, and is calculated as the percentage of the hourly wind data representing westerly winds, with those indicating easterly winds subtracted. This hypothesis that wind directions will be affected, is supported by our good relationship between the WWF and O_{x_bkg} at the Baengnyeongdo site, which is closest to the Asian continent.

Fig. 9b shows that the WWF is in good correlation with O_{x_bkg}. The averaged O_{x_bkg} level (46 ppb) at the three sites is also comparable to the observed O_x at Baengnyeongdo (51 ppb) during the same period (2015–2017) (Fig. 3c). In addition, the y intercept value for the WWF–O_{x_bkg} regression line in Fig. 9b indicates the level at which WWF becomes zero, implying no impact from LRT (denoted as $O_{x\_bkg\_noLRT}$). The level of $O_{x\_bkg\_noLRT}$ in our study was estimated to be 34 ppb as shown in Fig. 9b. The difference between O_{x_bkg} and $O_{x\_bkg\_noLRT}$ can be attributed to an LRT contribution (~27%) from the Asian continent. This range also corresponds to the previous modeled values of 28–38% (Chou et al., 2009), 22.8–34.8% (Nagashima et al., 2010), and 5–20% (Li et al., 2016).

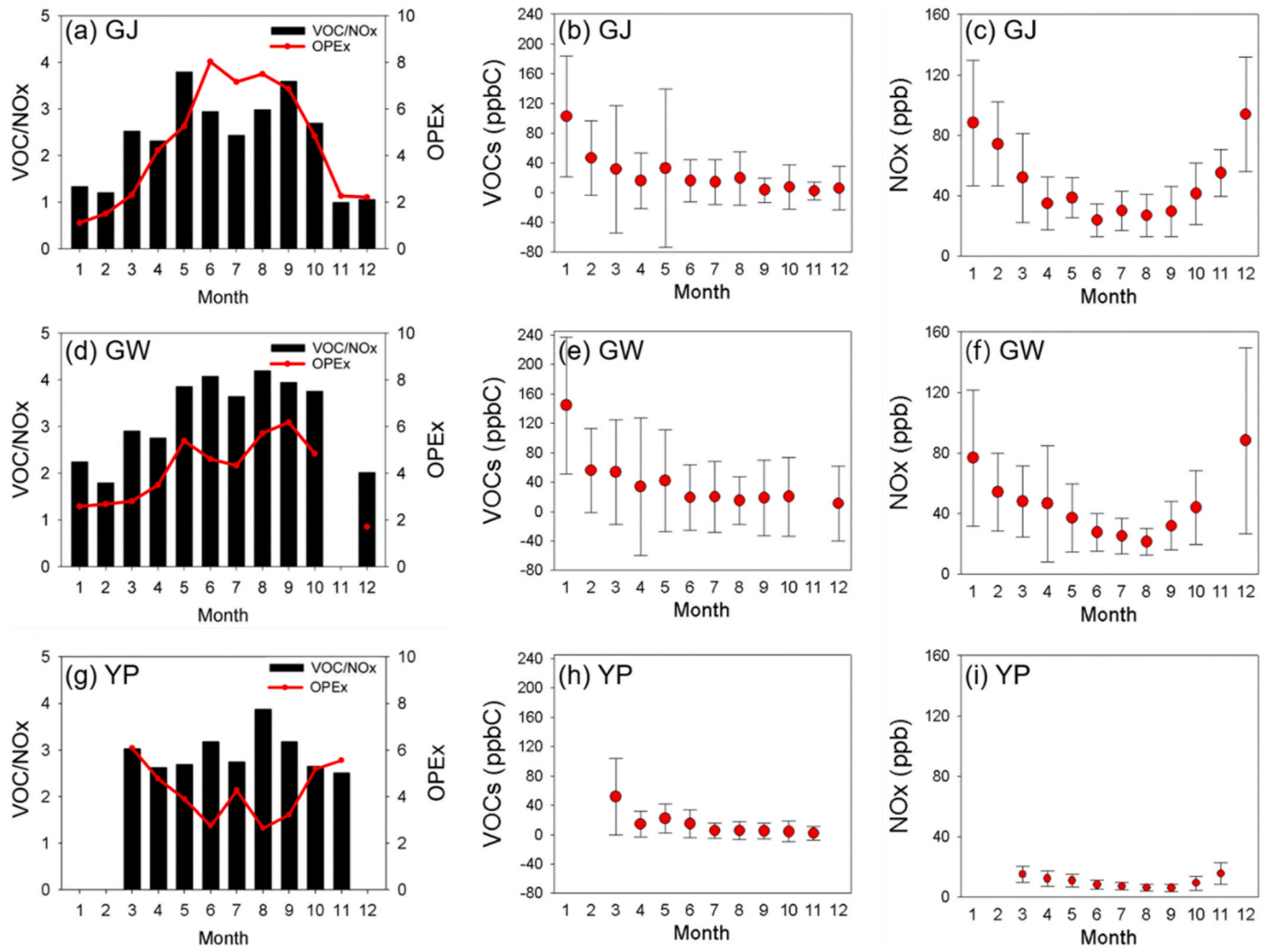

Fig. 7. Comparison of monthly variations in OPE_x, VOC/NO_x ratios, VOCs, and NOx at Gwangjin (GJ) (a–c), Guwol (GW) (d–f), and Yangpeong (YP) (g–i) for selected days following the criteria described in the methods section.

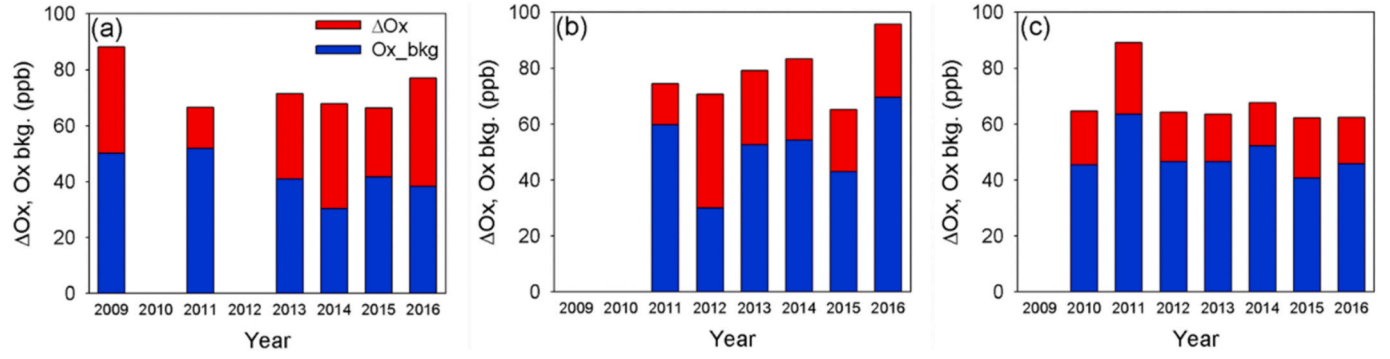

Fig. 8. Annual mean ΔO_x (red), O_x_bkg (blue), and O_x ($=\Delta O_x + O_x$_bkg) at (a) Gwangjin (GJ), (b) Guwol (GW), and (c) Yangpeong (YP). (For interpretation of the references to colour in this figure legend, the reader is referred to the Web version of this article.)

3.3. Response of O_x to NO_2 emission changes

Starting with the first Ten-Year Plan, which introduced special control measures in the SMA for 2005–2014 (ME, 2005), Korea has enacted policies to reduce NO emissions from industry, vehicles, and other sources. The Korean government set a goal of reducing NO_2 emissions by 53% during this period, with the aim of reaching an NO_2 value of 22 ppb. We inferred the response of O_x to NO_2 emission changes through the relationship of the two O_3 components (O_{x_bkg} and ΔO_x) with NO_x, OPE_x, and NO_z in the SMA.

Fig. 10 shows scatter plots for OPE_x, NO_x, NO_z, O_x_bkg, and ΔO_x at the three PAMS sites. The scatter diagram for OPE_x and NO_x is separated into high and low NO_x zones by a threshold value of approximately 10 ppb. It can be seen that OPE_x is inversely proportional to NO_2 in the high-NO_2 zone, while it is directly proportional to NO_2 in the low-NO_2 zone. An inverse relationship between OPE_x and NO_2 has also been

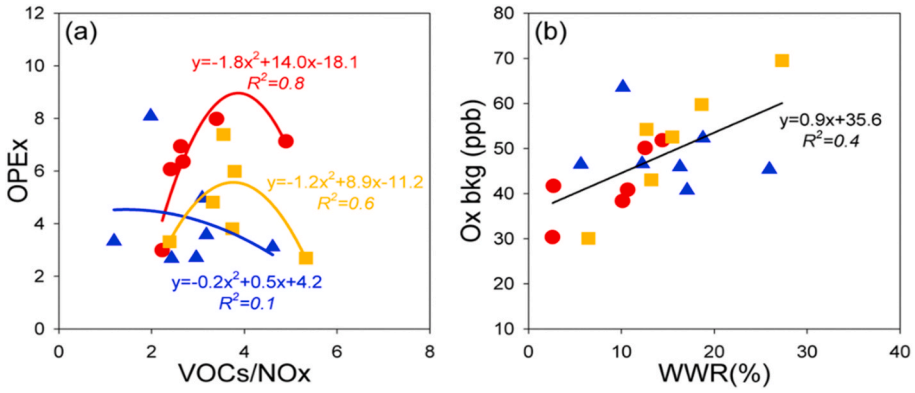

Fig. 9. Scatter plots of annual means of (a) OPE_x versus $VOCs/NO_x$ and (b) background O_x concentrations versus west wind fraction (%) at GJ (red circles), GW (yellow rectangles), and YP (blue triangles). Linear fitting parameters (slope and R^2) are also shown. (For interpretation of the references to colour in this figure legend, the reader is referred to the Web version of this article.)

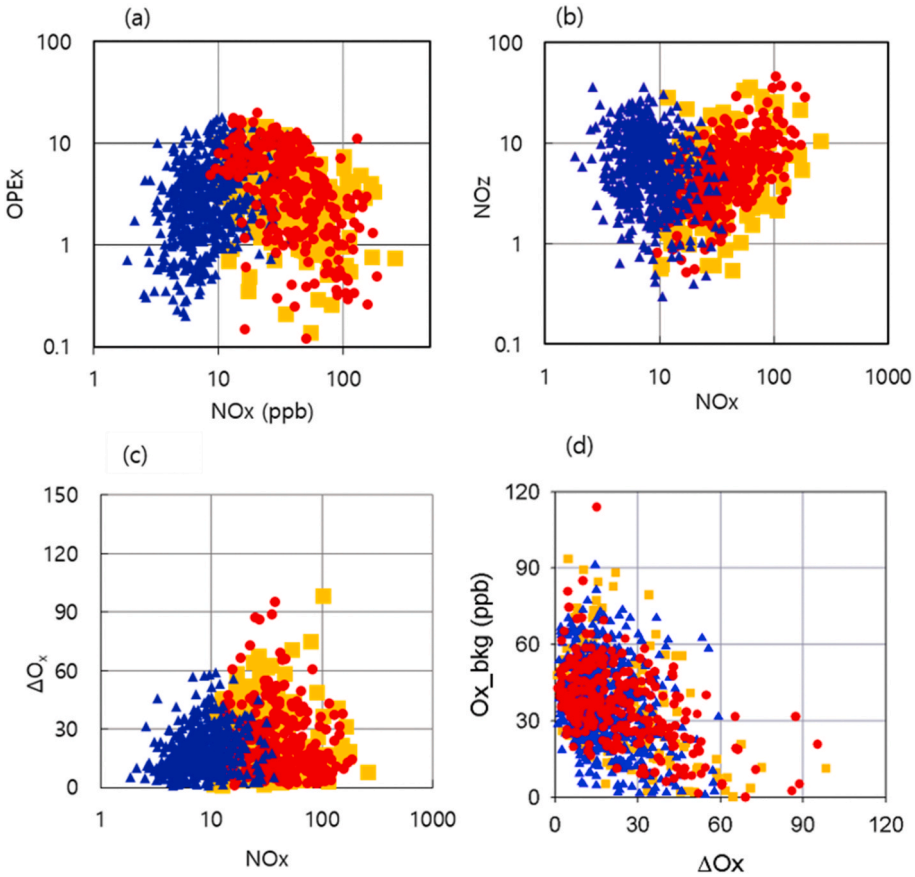

Fig. 10. Scatter plots of (a) observed daily means OPE_x versus NO_x, (b) NO_z versus NO_x, (c) ΔO_x versus NO_x, and (d) O_{x_bkg} versus OPE_x at GJ (red circles), GW (yellow rectangles), and YP (blue triangles) for selected days following the criteria described in the methods section. (For interpretation of the references to colour in this figure legend, the reader is referred to the Web version of this article.)

reported in several studies (Chou et al., 2009; Lei et al., 2007), but a proportional relationship under low-NO_x conditions has, to our knowledge, very rarely been investigated. Similar results were obtained from a model-based estimation of OPE_x versus NO_x in Houston (Mazzuca et al., 2016). However, an observational study at a rural site in New York state (Ninnenman et al., 2017) showed that OPE_x rapidly decreases when NO_x increases, which is in opposition to our results. Thus, we can assume that the OPE_x–NO_2 relationship can differ depending on the O_3 regime, and more work is needed to characterize the dependence of OPE_x on NO_x in low-NO_x environments.

The scatter plot of NO_x versus NO_z is also separated into two groups, but their relationship is opposite to that of OPE_x versus NO_x. When the level of NO_x is reduced, OPE_x increases (decreases) while NO_z decreases (increases) at urban (suburban) sites. As an increase (decrease) in OPE_x resulting from decreased NO_x concentrations would be offset by a NO_z decrease (increase), the overall relationship between ΔO_x (= $OPE_x \times NO_z$) and NO_x becomes less clear. On the other hand, ΔO_x generally shows a negative relationship with the regional background O_3 concentration of approximately 10 ppb or more. This is due to the fact that when the regional background concentration decreases below a certain

level, the regional background significantly suppresses photochemical production. Considering recent studies showing that Northeast Asia has a relatively higher O_3 background than Europe and America, we can infer that the regional background becomes an important factor for the development of an O_3 control strategy in the SMA.

Overall, in urban areas, a decrease in NO_2 leads to an increase in OPE_x through potential O_3 formation. However, the increase in OPE_x is sufficiently offset by a decrease in NO_z. In this manner, changes in O_x would be insignificant despite marked changes in NO_2. In contrast, at the suburban site, decreased NO_2 level led to decreased OPE_x and increased NO_z, and as a result, induced an increase in ΔO_x with no discernible change in NO_z, consequently suppressing photochemical O_x production. Together, these results therefore suggest that urban O_3 policies should consider significant cuts in NO_x emissions to allow the O_3 regime to shift (Kim et al., 2018).

4. Conclusions

The O_3 level in the SMA in Korea has steadily increased despite reductions in O_3 precursor emissions. It seems that decreases in NO_x resulted in increases in both the daily mean and peak O_3 levels in the SMA, which is attributed to weakened titration under a NO_x-titration regime. However, details of this process are rather complicated; a decrease in NO_x in the SMA leads to an increase in OPE_x, but this increase is accompanied by a decrease in NO_z, resulting in no discernible change in the total photochemical oxidant production. Meanwhile, regional background does not seem to significantly affect OPE_x, even though recent studies have reported that Northeast Asia has a relatively high O_3 background compared with other continents (Chang et al., 2017).

Marked reductions in NO_x emissions enable cities to switch from a VOC-limited to a NO_x-limited regime, which may have positive practical effects. For cities such as Ulsan that are already in a NO_x-limited regime, the O_3 problem may be alleviated solely by a reduction in NO_x emissions. In addition, when used concurrently with VOC reduction policies, NO_x reduction policies can successfully lower the overall photochemical oxidant level. Nevertheless, weak NO_x control regulations may be insufficient due to the complex behaviors of both OPE_x and NO_z.

For the public, the negative effects of O_3 are considerably more difficult to detect compared with those of other pollutants. Moreover, O_3 levels that trigger O_3 alerts or warnings occur mainly during the daytime, which heightens their potential health hazards. Thus, continuous efforts to reduce the emissions of O_3 precursors while considering the O_3 characteristics of a region are imperative for the protection of human health.

CRediT authorship contribution statement

Lim-Seok Chang: Conceptualization, Writing - original draft. **Jin-Young Choi:** Data curation. **Jongseok Son:** Investigation, Validation. **Sangbo Lee:** Data curation, Formal analysis. **Daegyun Lee:** Resources. **Yu-Jin Jo:** Visualization, Investigation. **Cheol-Hee Kim:** Supervision, Writing - review & editing.

Declaration of competing interest

The authors declare that they have no known competing financial interests or personal relationships that could have appeared to influence the work reported in this paper.

Acknowledgments

This work was supported by a grant from the National Institute of Environment Research (NIER), funded by the Ministry of Environment (MOE) of the Republic of Korea (NIER-2018-01-01-028). C.-H. Kim (corresponding author) acknowledge partial supports made by National Research Foundation of Korea (NRF) funded by the Ministry of Education of the Republic of Korea (Grant No. 2020R1A6A1A03044834). Also thanks are given to three anonymous reviewers for their helpful comments.

Appendix A. Supplementary data

Supplementary data to this article can be found online at https://doi.org/10.1016/j.atmosenv.2020.117846.

References

Bowman, F.M., Seinfeld, J.H., 1994. Ozone productivity of atmospheric organics. J. Geophys. Res. 99 (No. D3), 5309–5324.

Chang, K.L., Petropavlovskikh, I., Cooper, O.R., Schultz, M.G., Wang, T., 2017. Regional Trend analysis of surface ozone observations from monitoring networks in eastern North America, Europe and East Asia. Elem. Sci. Anth. 5, 50. https://doi.org/10.1525/elementa.243.

Choi, K.-C., Lee, J.-J., Bae, C H, Kim, C.-H., Kim, S., Chang, L.-S., Ban, S.-J., Lee, S.-J., Kim, J., Woo, J.-H., 2014. Assessment of transboundary ozone contribution toward South Korea using multiple source-receptor modeling techniques. Atmos. Environ. 92, 118–129. https://doi.org/10.1016/j.atmosenv.2014.03.055.

Chou, C.C.K., Tsai, C.Y., Shiu, C.J., Liu, S.C., Zhu, T., 2009. Measurement of NO_y during campaign of air quality research in Beijing 2006 (CAREBeijing-2006): implications for the ozone production efficiency of NO_x. J. Geophys. Res. 114, D00G01. https://doi.org/10.1029/2008JD010446.

European Commission, 1999. Ozone position paper. https://ec.europa.eu/environment/archives/air/pdf/documents/pos_paper.pdf.

Friedrich, R., Reis, S. (Eds.), 2000. Tropospheric Ozone Abatement: Developing Efficient Strategies for the Reduction of Ozone Precursor Emissions in Europe. Springer Berlin Heidelberg. https://doi.org/10.1007/978-3-642-59698-8.

Godowitch, J.M., Pouliot, G.A., Rao, S.T., 2010. Assessing multi-year changes in modeled and observed urban NO_x concentration from a dynamic model evaluation perspective. Atmos. Environ. 44 (24), 2894–2901. https://doi.org/10.1016/j.atmosenv.2010.04.040.

Ge, B.Z., Xu, X.B., Lin, W.L., Li, J., Wang, Z.F., 2012. Impact of the regional transport of urban Beijing pollutants on downwind areas in summer: ozone production efficiency analysis. Tellus B 64, 1. https://doi.org/10.3402/tellusb.v64i0.17348.

Haagen-Smit, A.J., Fox, M.M., 1953. Ozone formation in photochemical oxidation of organic substances. Ind. Eng. Chem. 48 (9), 1484–1487. https://doi.org/10.1021/ie51400a033.

Han, J.H., Kim, H.Y., Lee, M.H., Kim, S.Y., Kim, S.W., 2013. Photochemical air pollution of Seoul in the last three decades. J. Korean Soc. Atmos. Environ. 29, 390–406. https://doi.org/10.5572/KOSAE.2013.29.4.390.

Han, J.S., Moon, K.J., Kim, R.H., Shin, S.A., Hong, Y.D., Jung, I.R., 2000. Preliminary source apportionment of ambient VOCs measured in Seoul Metropolitan area by positive matrix factorization (Korean with English abstract). J. Korean Soc. Atmos. Environ. 22 (1), 85–97.

Hirsch, A.I., Munger, J.W., Jacob, D.J., Horowitz, L.W., Goldstein, A.H., 1996. Seasonal variation of the ozone production efficiency per unit NO_x at Harvard Forest, Massachusetts. J. Geophys. Res. 101, 12659–12666. https://doi.org/10.1029/96jd00557.

Jacob, D.J., Horowitx, L.W., Munger, K.W., Heikes, B.G., Dickerson, R.R., Artz, R.S., Keene, W.C., 1995. Seasonal transition from NO_x-to Hydrocarbon-limited conditions for ozone production over the eastern United States in September. J. Geophys. Res. 100, 9315–9324. https://doi.org/10.1029/94JD03125.

Kim, J., Ghim, Y.S., Han, J.S., Park, S.M., Shin, H.Y., Lee, S.B., Kim, J., Lee, G., 2018. long-term trend analysis of Korean air quality and its implication to current air quality policy on ozone and PM10. J. Korean Soc. Atmos. Environ. 34, 1–15. https://doi.org/10.5572/KOSAE.2018.34.1.001.

Kim, C.-H., Kim, Y.-K., Lee, H.W., Seo, K.-H., 2009. Simple method for simulating horizontal ozone concentration fields over coastal areas: A case study of the Seoul metropolitan area, Korea. Terr. Atmos. Ocean. Sci. 20, 355–363.

Kim, C.-H., Park, S.-U., Song, C.-K., 2005. A simple semi-empirical photochemical model for the simulation of ozone concentration in the Seoul metropolitan area in Korea. Atmos. Environ. 39, 5597.

Kleinman, L., Lee, Y., Springston, S.T., Nunnermacker, L., Zhou, X., Brown, R., Hallock, K., Klotz, P., Leahy, D., Lee, J.H., Newman, L., 1994. Ozone formation at a rural site in the southeastern United States. J. Geophys. Res. 99, 3469–3482. https://doi.org/10.1029/93JD02991.

Lee, C.B., Hwang, G.J., 2005. Evaluation of VOCs emissions using PAMS data and Model-3/CMAQ. J. Korean Soc. Atmos. Environ.

Lei, W., de Foy, B., Zavala, M., Volkamer, R., Molina, L.T., 2007. Characterizing ozone production in the Mexico City Metropolitan Area: a case study using a chemical transport model. Atmos. Chem. Phys. 7, 1347–1366. https://doi.org/10.5194/acp-7-1347-2007.

Li, J., Wang, W., Wang, Z., Chen, H., Hu, B., Li, J., Sun, Y., Fu, P., Zhang, Y., 2016. Modeling study of surface ozone source-receptor relationships in East Asia. Atmos. Res. 167, 77–88. https://doi.org/10.1016/j.atmosres.2015.07.010.

Marr, L.C., Harley, R.A., 2002. Spectral analysis of weekday weekend differences in ambient ozone, nitrogen dioxide, and non-methane hydrocarbon time series in

California. Atmos. Environ. 36, 2327–2335. https://doi.org/10.1016/S1352-2310(02)00188-7.

Mazzuca, G.M., Ren, X., Loughner, C.P., Estes, M., Crawford, J.H., Pickering, K.E., Weinheimer, A.J., Dickerson, R.R., 2016. 2013 Ozone production and its sensitivity to NOx and VOCs: results from the DISCOVER-AQ field experiment Houston. Atmos. Chem. Phys. 16, 14463–14474. https://doi.org/10.5194/acp-16-14463-2016.

ME, 2005. 1st Seoul Metropolitan Air Quality Control Master Plan (2005-2014). Ministry Environment of Korea. http://eng.me.go.kr/eng/web/index.do?menuld=235&findDepth=1.

Na, K., Kim, Y.P., 2001. Seasonal characteristics of ambient volatile organic compounds in Seoul, Korea. Atmos. Environ. 35, 2603–2614. https://doi.org/10.1016/S1352-2310(00)00464-7.

Nagashima, T., Ohara, T., Sudo, K., Akimoto, H., 2010. The relative importance of various source regions on East Asian surface ozone. Atmos. Chem. Phys. 10, 11305–11322. https://doi.org/10.5194/acp-10-11305-2010.

National Air Pollutant Emission Service(NAPES), 2016. Retrieved. http://airemiss.nier.go.kr/. (Accessed 1 July 2019).

National Research Council (NRC), 1991. Rethinking the Ozone Problem in Urban and Regional Air Pollution. Natl. Acad. Press, pp. 109–186. https://doi.org/10.17226/1889.

Ninnenman, M., Lu, S., Lee, P., McQueen, J., Huang, J., Demerjian, K., Schwab, J., 2017. Observed and Model-derived ozone production efficiency over urban and rural New York State. Atmosphere 8, 126. https://doi.org/10.3390/atmos8070126.

Oak, Y.J., Park, R.J., Schroeder, J.R., Crawford, J.H., Blake, D.R., Weinheimer, A.J., Woo, J.H., Kim, S.W., Yeo, H., Fried, A., Wisthaler, A., Brune, W.H., 2019. Evaluation of simulated O3 production efficiency during the KORUS-AQ campaign: implications for anthropogenic NOx emissions in Korea. Elem Sci Anth 7, 56. https://doi.org/10.1525/elementa.394.

Sillman, S., 1993. Tropospheric ozone: the debate over control strategies. Annu. Rev. Energy Environ. 18 (1), 31–56. https://doi.org/10.1146/annurev.eg.18.110193.000335.

Sadanaga, Y., Matsumoto, J., Kajii, Y., 2003. Photochemical reactions in the urban air: recent understandings of radical chemistry. J. Photochem. Photobiol. C Photochem. Rev. 4 (1), 85–104. https://doi.org/10.1016/s1389-5567(03)00006-6.

Susaya, J., Kim, K.H., Shon, Z.H., Brown, R.J., 2013. Demonstration of long-term increase in tropospheric O_3 levels: causes and potential impacts. Chemosphere 92, 1520–1528. https://doi.org/10.1016/j.chemosphere.2013.04.017.

Tang, G., Li, X., Wang, Y., Xin, J., Ren, X., 2009. Surface ozone trend details and interpretations in Beijing, 2001–2006. Atmos. Chem. Phys. 9, 8813–8823. https://doi.org/10.5194/acp-9-8813-2009.

U.S. Environmental Protection Agency, 2006. Air Quality Criteria for Ozone and Related Photochemical Oxidants (Final Report, 2006). U.S. Environmental Protection Agency, Washington, DC. EPA/600/R-05/004aF-cF.

Zanis, P., Ganser, A., Zellweger, C., Henne, S., Steinbacher, M., Staehelin, J., 2007. Seasonal variability of measured ozone production efficiencies in the lower free troposphere of Central Europe. Atmos. Chem. Phys. 7, 223–236. https://doi.org/10.5194/acp-7-223-2007.